AIAA JOURNAL
Vol. 41, No. 5, May 2003

Application of Proper Orthogonal Decomposition to a Supersonic Axisymmetric Jet

E. Caraballo,* M. Samimy,† and J. Scott‡
The Ohio State University, Columbus, Ohio 43210
S. Narayanan§
United Technologies Research Center, East Hartford, Connecticut 06108
and
J. DeBonis¶
NASA John H. Glenn Research Center at Lewis Field, Cleveland, Ohio 44135

Results are presented from the application of the snapshot proper orthogonal decomposition (POD) method to a spatiotemporal flowfield generated from large eddy simulations (LES) of a Mach 1.4 ideally expanded jet. This is part of ongoing research in the development and use of the POD method in conjunction with advanced laser-based optical measurements in high-speed flows. The POD application goal is twofold: to extract dynamically significant information on the large-scale coherent structures in a high-speed jet and to facilitate low-dimensional modeling of the jet. It was found that the spatial eigenmodes obtained using weakly correlated snapshots, but spanning tens of convective timescale and uncorrelated snapshots, are similar. It was also found that a short-duration temporally resolved LES data (simulating data obtainable from pulse burst laser-based measurements) could be used to calculate the time evolution coefficients of the eigenmodes. The use of a few modes (namely, 12) was sufficient for a reasonable reconstruction of the spatiotemporal flowfield. The use of POD with a vector norm instead of a scalar norm did reduce the energy captured in the first few modes and also changed their rank order, but did not substantially alter the reconstructed flow. In the early jet development region, the first and dominant mode was found to be axisymmetric, followed by either another axisymmetric or asymmetric (probably helical) mode, whereas higher modes in this region and all of the modes farther downstream were more complex and three-dimensional. The POD modes and their temporal coefficients obtained at various streamwise locations suggest that the large-scale jet structures undergo a process of disorganization near the end of potential core, followed by reorganization farther downstream.

Nomenclature

A	=	matrix of the intermediate eigenvalue problem [Eq (2)]
$a^n(t)$	=	random temporal coefficient of the nth POD eigenvalues [Eq. (5)]
$C(t, t_k)$	=	two-point correlation tensor of independent snapshots [Eq. (3)]
D	=	nozzle exit diameter
M	=	total number of snapshots
n	=	mode number
r	=	nozzle exit radius
T_s	=	time step
t, t_k	=	time
u_i	=	velocity components
x	=	streamwise coordinate
$\boldsymbol{x}$	=	(x, y, z) Cartesian coordinates
λ^n	=	nth POD eigenvalue
φ^n	=	eigenfunction corresponding to the nth POD eigenvalue
$(,)$	=	inner product

Received 18 December 2001; revision received 4 December 2002; accepted for publication 17 December 2002.

*Graduate Student, Gas Dynamics and Turbulence Laboratory, Department of Mechanical Engineering. Student Member AIAA.
†Professor and Director, Gas Dynamics and Turbulence Laboratory, Department of Mechanical Engineering; Samimy.1@osu.edu. Associate Fellow AIAA.
‡Associate Professor, Aerospace and Aviation Department. Associate Fellow AIAA.
§Associate Fellow, Systems Department. Member AIAA.
¶Aerospace Engineer, Nozzle Branch. Senior Member AIAA.

Introduction

IT has been known for decades that large-scale coherent structures play a major role in many engineering applications. Examples include entrainment and mixing in mixers and combustors, noise generation in jets, and drag in moving vehicles. There is a consensus that an effective way to control these processes is to control large-scale (coherent) structures. However, there is a great deal of debate and subjectivity in defining a coherent structure and its identification via experiments or numerical simulation.

The proper orthogonal decomposition (POD) method is an empirical mathematical tool, introduced to turbulence research by Lumley, that objectively identifies dynamically significant structures in the flow.[1] The technique is empirical in that it uses a spatial velocity correlation tensor that is obtained experimentally or from numerical simulations. This correlation tensor is sufficient for identifying various eigenmodes supported by the flow. However, to go one step beyond and to investigate temporal evolution of large-scale structures, one needs to project these modes onto real-time experimental or computational data.[2] One can also use Galerkin methods to project Navier–Stokes equations onto these eigenmodes to derive a set of ordinary differential equations that can predict, at least in a global sense, the flow behavior. These ordinary differential equations may then be used for closed-loop flow control.[3]

The POD method has been used in the past decade to study coherent structures in various turbulent flows. For example, it has been used to study the wall region of a turbulent boundary layer,[4] low-subsonic axisymmetric jets,[5–7] a high-subsonic axisymmetric jet,[8] and in the developing region[9] and in the self-similar region[10] of a low-subsonic planar mixing layer. All of these applications of

POD have been in subsonic flows, and hot-wire probes have been used to obtain experimental data. Hot wires provide temporally well resolved but spatially sparse data for POD.

In recent years, the POD method has also been used with numerical simulation data. For example, it has been used to explore dynamics of flow separation in a diffuser over a range of expansion angles,[11] in both subsonic[12,13] and supersonic[14,15] cavity flows, and in a high-subsonic jet.[16]

Recent developments in optical diagnostic techniques such as particle image velocimetry and planar Doppler velocimetry (PDV) have enabled the acquisition of the required statistical data nonintrusively and with higher spatial resolution.[17] However, their use with the POD method has been limited because they do not provide temporally resolved data. Developments in laser and camera technologies and the associated real-time optical diagnostic techniques[18,19] provide a new impetus for the use of POD with planar laser-based optical techniques.

High-speed, high-Reynolds number jets are relevant to commercial and military engineering applications, and an understanding of their physics is, therefore, critical. The use of hotwires in such flows would be quite challenging. Our approach is to use the POD method with experimental data obtained from the PDV technique. PDV will provide planar images with three velocity components at a large number of spatial points, but with no time correlation between the images. Additionally, it is becoming possible to obtain a series of real-time single velocity components with short time duration using a real-time PDV technique under development.[18,19] This paper presents the first step in the development and application of POD with PDV-type laser-based diagnostics data.

POD Approach

The POD method is a mathematical tool used to decompose a data set, which contains information on all or at least on most scales of a turbulent flow, into a small number of modes that can capture the dynamically significant structures in the flow. It has been used as an objective method to identify coherent structures in turbulent shear flows.[1] The method provides a spatial basis (a set of eigenfunctions) for a modal decomposition of an ensemble of data, obtained from an experiment or computational simulations. These eigenfunctions, or modes, are extracted from the cross-correlation tensor and can be used as basis functions to represent the flow. It is generally accepted that the empirical eigenfunctions obtained from the POD method and the coherent structures in the flowfield are related. Lumley noted that if the first mode contains a dominant percentage of the fluctuating energy, it could represent a physical structure.[20] However, for flows requiring several modes for adequate energy capture, the POD modes provide a good spatial basis for flow decomposition, but the connection between these modes and the physical-space coherent structures in the flow is not clear.

Details of the POD approach have been provided by several investigators and will not be repeated here.[1,2,4,6,14,21,22] The method used in the present work is the snapshot method developed by Sirovich.[2] The snapshot method is more suitable to obtain the POD modes in highly spatially resolved data sets because the classical method is computationally intensive. The method requires a sufficiently large number, $k = 1, 2, \ldots, M$, of instantaneous realizations or snapshots, $u_i(\boldsymbol{x}, t_k)$, for a statistically stationary representation of the flow. Then the POD eigenfunctions can be written as linear combinations of the instantaneous flowfields:

$$\varphi^n(\boldsymbol{x}) = \sum_{k=1}^{M} A_k u(\boldsymbol{x}, t_k) \tag{1}$$

The eigenfunctions can be obtained by solving the following eigenvalue problem:

$$C(t, t_k)A = \lambda^n A \tag{2}$$

where the matrix A is the eigenbasis of this intermediate eigenvalue problem and $C(t, t_k)$ is the two-point correlation tensor of the snapshots, integrated over the spatial domain of interest or spatial average of the correlation tensor, defined as

$$C(t, t_k) = \frac{1}{M} \int_D u_i(\boldsymbol{x}, t) u_i(\boldsymbol{x}, t_k)\, \mathrm{d}\boldsymbol{x} \tag{3}$$

This procedure reduces the eigenvalue problem from one that depends on the number of grid points to one that depends only on the number of snapshots M used. Additionally, the snapshot method does not need to invoke the spatial homogeneity assumption.

The instantaneous velocity field can then be reconstructed using the eigenfunctions, as

$$u_i(\boldsymbol{x}, t) = \sum_{n=1}^{\infty} a^n(t) \varphi_i^n(\boldsymbol{x}) \tag{4}$$

where a^n are the random temporal coefficients that can be calculated from

$$a^n(t) = \int_D u_i(\boldsymbol{x}, t) \varphi_i^{n*}(\boldsymbol{x})\, \mathrm{d}\boldsymbol{x} \tag{5}$$

Time-resolved velocity data are not available, in general. The time coefficients must be obtained by other means such as Galerkin projection of Navier–Stokes equations onto the eigenfunctions.

The objective of the present study was to explore the feasibility of using POD with the experimental data that can be obtained using the PDV technique. The standard PDV technique can provide highly spatially resolved instantaneous velocity and detailed statistical data on any given plane, but it cannot provide time-resolved data, due to the shortcomings of both current commercial lasers and charge-coupled device (CCD) cameras.[17] A technique based on pulse burst laser with a repetition rate of up to 1 MHz and an ultrafast CCD camera with similar frame rate is under development.[18,19] Currently, this imaging system is limited to recording 17 consecutive images on the camera for a 150-μs pulse burst span from the laser. A question, therefore, was, could this kind of limited data be used with POD technique to provide information on dynamics of coherent structures for their control?

To assess the feasibility of POD application to PDV data, data obtained using large eddy simulations (LES)[23,24] were used. LES resolves a large portion of the spatial scales and associated temporal scales in the flows considered. Therefore, LES data have very high spatial resolution, which is, in a sense, similar to data from PDV, while providing good time resolution (not currently available via PDV).

LES Database

The data used here were obtained from a three-dimensional LES of a high-Reynolds-number supersonic jet.[23,24] The LES code[25] combines a five-stage, fourth-order Runge–Kutta time discretization[26] with a standard fourth-order central difference spatial discretization. Stability is maintained by removing high wave number dispersive errors with a sixth-order explicit filter.[26] A compressible form of the Smagorinsky model is used to represent the subgrid scale stresses (see Ref. 27). The flow was a Mach 1.4 ideally expanded axisymmetric jet issuing from a 2.54-cm-diam nozzle. The computational domain included both the jet flowfield and the nozzle geometry. This allows for a realistic development of the jet mixing layer, by providing an accurate representation of the flow conditions at the nozzle exit and the initial jet velocity profile. The computational domain extends 20 jet diameters ($20D$) from the nozzle exit in the streamwise direction and $10D$ from the centerline in the radial direction. The computational grid was formed by 301 points in the x direction (streamwise), 129 points in the radial direction, and 36 points in the azimuthal direction. The grid size in the axial and radial directions was determined from a grid study with preliminary axisymmetric solutions.[28] A grid resolution study for the azimuthal direction found only slight differences in time-averaged quantities between the 36-plane solution presented here and a finer 64-plane solution.[23]

Figure 1 shows the computational grid used in the LES for a cross-stream and for the streamwise planes. In the cross-stream plane (Fig. 1a), only the region contained within $r = 1D$ is shown. The streamwise plane (Fig. 1b) shows the grid only downstream of the

nozzle. The grid is nonuniform in the radial direction y, as well as in the streamwise direction x with a finer grid distribution in the mixing-layer region. The time step used in the simulation was 5×10^{-8} s. For the snapshot POD analysis used here, data at an interval of 80 time steps were used (4×10^{-6} s). The data used were for three cross-stream (y–z) planes at $3D$, $6D$, and $9D$. DeBonis and Scott[23] compared time-averaged velocity profiles, both centerline and radial, with the experimental data.[29] The computation underpredicts the length of the potential core by about 1.5 jet diameters and, beyond this point, the jet spreads at a slightly higher rate. The prediction of the potential core length represents a 50–70% improvement over comparable LES. Two-point space–time correlations, performed near the end of the potential core, indicate that the convection speed of the large-scale turbulent structures is in agreement with the stream selection rule.[18] Although there is a need for improvement in accuracy, this calculation is an advance in the unsteady analysis of high-Reynolds-number jets and is the most suitable for the present POD analysis.

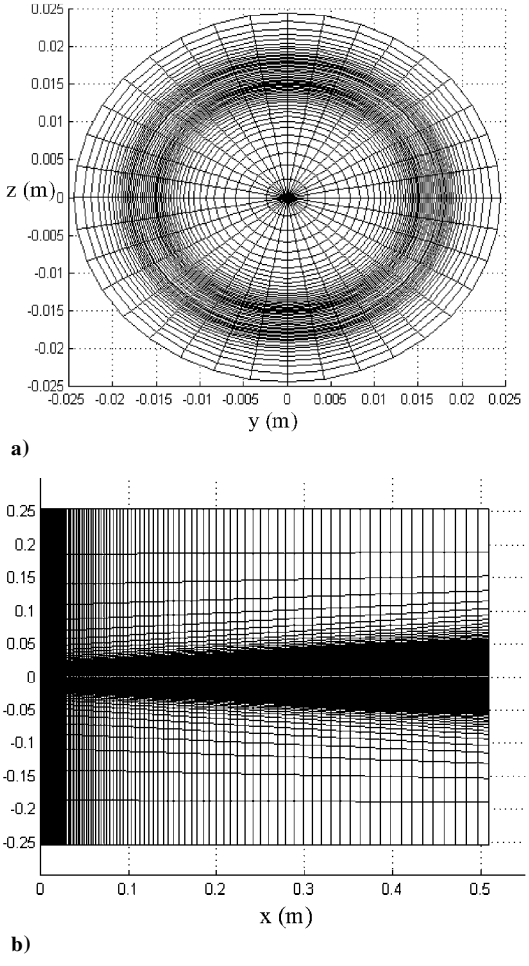

Fig. 1 Computational grid used in the LES code: a) cross-section plane and b) streamwise plane (note that the scales for panels a and b are different).

Results and Discussion

The POD method was applied to the LES data at the cross-stream planes just described. The results can be put into three categories: 1) those that deal with issues such as the energy content of each mode and the numbers of modes required to reconstruct the flowfield, 2) those that explore the nature and dynamics of the large-scale structures in a high-speed jet, and 3) those that assess the applicability of the POD method with the type of data that can be obtained using PDV (namely, well-resolved data fields in space but resolved over a short time span). Although the LES data contain the full volumetric information, that is, three velocity components, density, and pressure, at every time step, we will limit our discussions to two-dimensional cross-sections and three components of velocity, similar to what will be available experimentally using PDV.

POD Modes

The LES data at $x/D = 3$, 6, and 9 contained a total of 850 data sets or snapshots (every 80th computational time step is a snapshot) at each location. Assuming a convective velocity of 300 m/s and a length scale of one nozzle exit diameter (2.54 cm), the convective timescale is 85 μs, whereas the time interval at which the snapshots were sampled was 4 μs (the simulations time step was 0.05 μs). Therefore, the available total data length was approximately 40 convective timescale for $x/D = 9$ location and almost 100 convective timescale for $x/D = 3$, which contains a statistically significant number of coherent structure passages. Reduced sets of at least 100 snapshots, using one from out of every five to eight snapshots, distributed over the entire 850 snapshots available, were used to calculate the POD basis at each section. From now on, these sets will be referred to as the "ordered data set." Statistical convergence in the percentage of energy captured by the modes was observed.[30] Although in these data sets two consecutive snapshots are weakly correlated, each data set spans 40–100 convective time units, over which the flow processes are decorrelated.

Figure 2 shows the percentage of captured energy (contained in the streamwise velocity fluctuations only) vs the number of POD modes at each cross-stream plane. The first POD mode contains 39, 17, and 31% of the energy at $x/D = 3$, 6, and 9, respectively. To capture 90% of the energy, the first 11, 16, and 14 modes are required at $x/D = 3$, 6, and 9, respectively. Interestingly, the percentage of energy captured by a given number of modes decreases from $3D$ to $6D$ and then increases at $9D$, and this variation is substantial for the first 20 modes or so. We speculate that this trend is a result of the following dynamics. Structures at $3D$, in the jet's early development region, are more coherent. At $6D$, around the end of the potential core, strong interactions between structures of

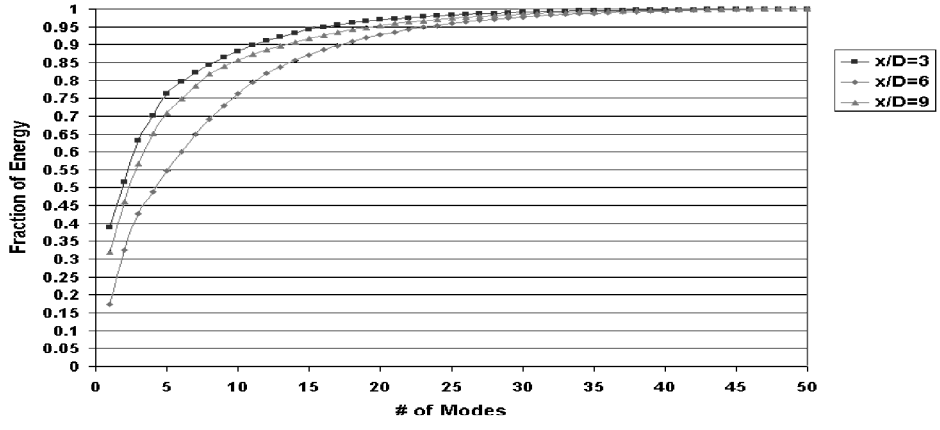

Fig. 2 Fraction of the energy captured by the POD modes at the three cross-stream planes.

merging shear layers take place, resulting in the loss of their organization. By $9D$, interactions between structures are not as strong and frequent. Therefore, they reorganize and become more coherent. Observations via temporally resolved flow visualizations of a Mach 1.3 ideally expanded, high-Reynolds-number jet, are consistent with this trend.[18] Similar observations have also been reported by others in a high subsonic axisymmetric jet.[8] Such reorganization of coherent structure dynamics in the far field of turbulent wakes has been studied via coherent structure eduction techniques.[31] However, no clear understanding of the physical mechanisms underlying this process is yet available. The implications of such processes on the mixing and noise generation process are not understood either.

When POD was used with the streamwise plane data, the first POD mode captured around 28, 17, and 38% of the energy in sections, which extend from $x/D = 1$-5, 4–8, and 7–11, respectively.[32] To recover 90% of the energy, it requires 21, 24, and 20 modes, respectively, at each section. Although the trend of captured energy is consistent with that obtained in the cross-stream planes, the modes extracted from such a plane do not account for three-dimensional structures and are quite different. Freund and Colonius[16] have showed that the nature of modes/structures and the convergence of associated eigenvalues are different when one uses volumetric or planar data for reconstruction of the modes.

In what follows, we will focus on the results that will reveal the dynamic significance of each mode and their streamwise evolution. For quantitative comparisons, reconstructed velocity time traces in the shear layer will be assessed to establish the minimum number of modes required to obtain a good representation of dynamically significant flow features and structures.

Spatial Structure of POD Modes

The characteristics of the POD modes at each cross-stream plane are now analyzed to explore the nature of the dynamically significant structures in the flow. In analyzing the modes, it should be kept in mind that each mode can be thought of as capturing a dominant flow characteristic that may or may not render itself to visualization or other diagnostic techniques. Figures 3–5 show the first six POD

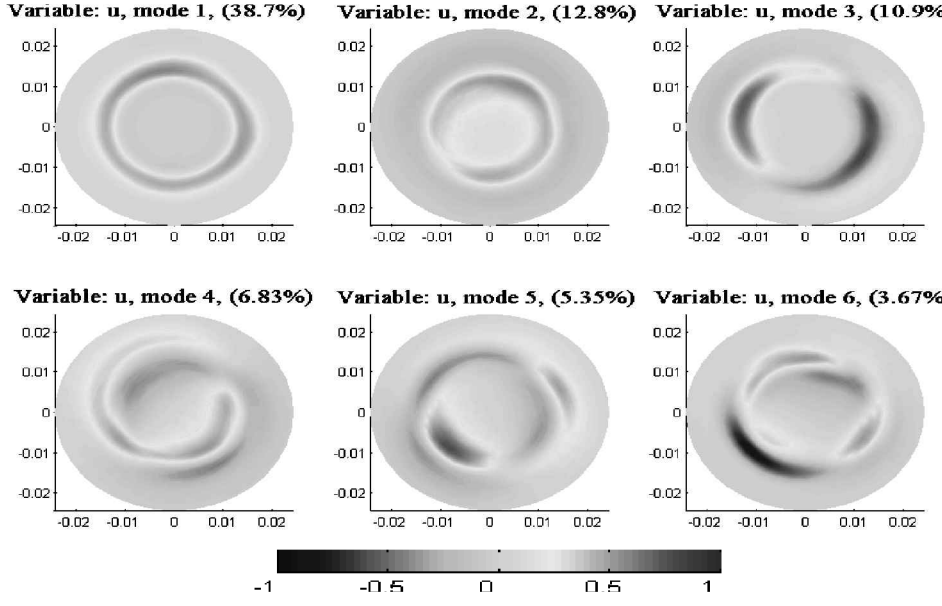

Fig. 3 First six POD modes for the streamwise velocity fluctuations at $x/D = 3$.

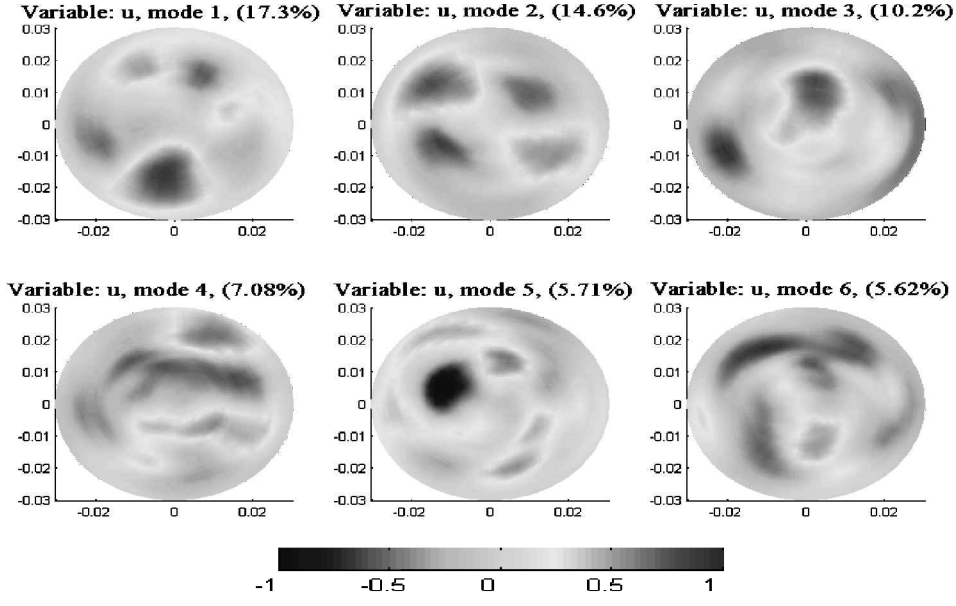

Fig. 4 First six POD modes for the streamwise velocity fluctuations at $x/D = 6$.

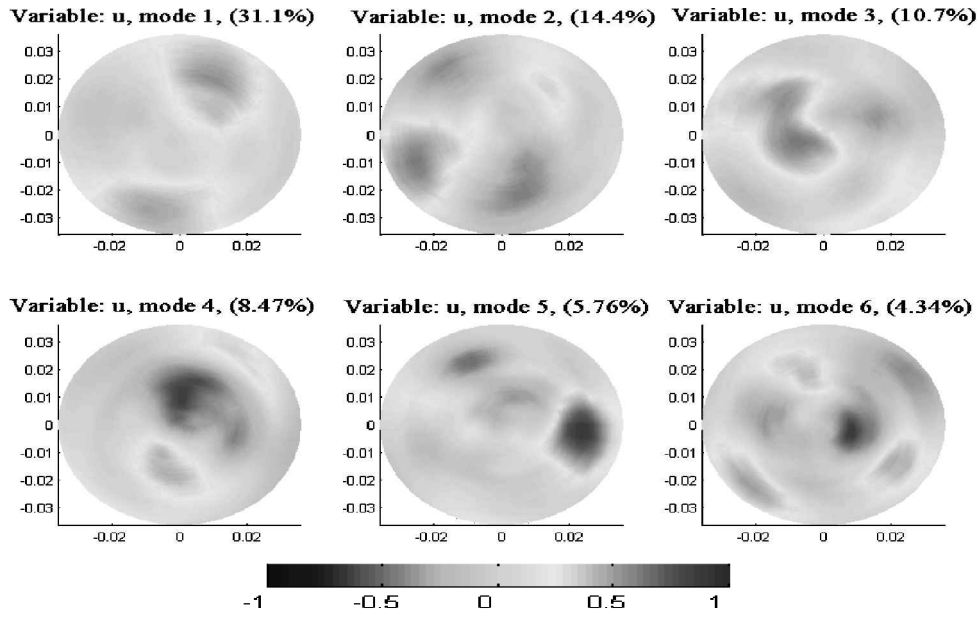

Fig. 5 First six POD modes for the streamwise velocity fluctuations at *x/D* = 9.

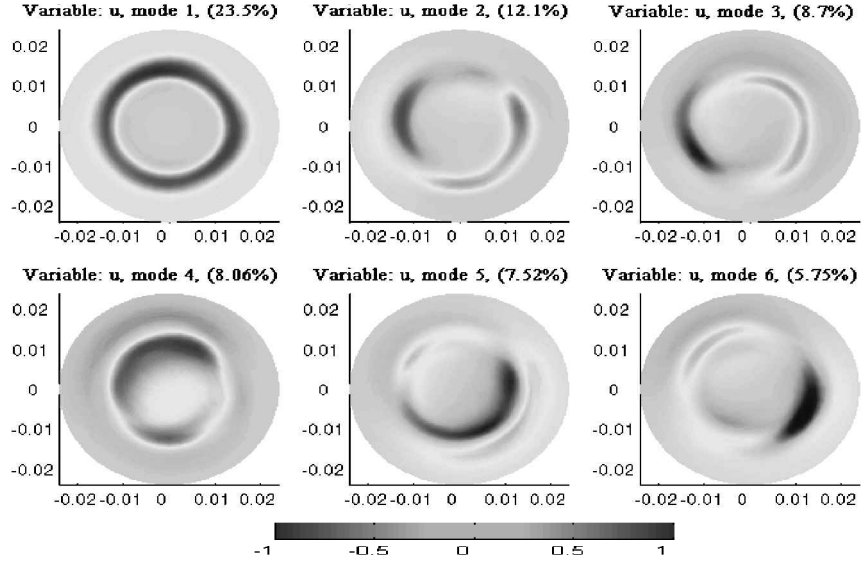

Fig. 6 First six POD modes for the streamwise velocity fluctuations at *x/D* = 3 using vector norm.

modes for the longitudinal velocity fluctuations at three cross-stream planes. For the cross-stream plane at $x/D = 3$, the first two modes are axisymmetric, showing a ring-type structure in the mixing-layer region. It is well known that in fully expanded jets, ring vortices dominate earlier in the mixing region. Recent real-time flow visualization in a similar Mach number jet show this feature clearly, with smaller-scale structures (mostly streamwise vortices) also riding on these large toroidal structures.[18] The third mode is asymmetric, evidently associated with the first azimuthal mode ($m = \pm 1$) with energy levels comparable to that for the second mode. Such azimuthal modes are known to be dominant farther downstream (close to the end of the jet potential core). Higher modes have more complex shapes and contain less energy.

At $x/D = 6$, even the first mode has a more complicated shape and is no longer the dominant mode, having comparable energy levels to that of the second mode, which has an asymmetric shape that can be associated with contributions from an $m = \pm 2$ mode. The higher modes have relatively high energy levels and complexity. This location is close to the end of the average potential core, where significant interactions occur among turbulence structures of the merging shear layers. These complex three-dimensional interactions, believed to be responsible for most of the far-field noise radiation,[33,34] are probably responsible for the reduced organization as well.

At the $x/D = 9$ plane, the energy distribution among the modes is similar to that at $x/D = 3$, where the first mode is dominant, although clearly three-dimensional in nature (compared to the axisymmetric structure near $x/D = 3$). The modes contain larger regions of positive and negative values while displaying greater spatial homogeneity. This is probably because the structures are quite large at this streamwise location and the associated turbulent kinetic energy is more evenly distributed over the cross section. The observed change in the shape of the first POD mode over the three cross-stream planes is similar to available experimental results in low-speed jets, which show that the flow structures are more axisymmetric in the developing jet region, that is, $x/D = 3$, but become more three-dimensional farther downstream.[35]

The POD modes were also calculated using a vector norm, which basically uses velocity vector rather than a single component of velocity.[13,16] Figure 6 shows the first six modes for the streamwise

velocity fluctuations at $x/D = 3$ calculated with this approach. It can be observed that the shape of the first mode is the same as in Fig. 3 but that the percentage of energy recovered has been reduced. Also there is a change in the order of the next three modes, where mode 2 in Fig. 3 appears as mode 4 in Fig. 6, and modes 3 and 4 in Fig. 3 as modes 2 and 3 in Fig. 6, respectively. However, the modes of the streamwise velocity fluctuations at the other two streamwise locations ($x/D = 6, 9$) did not show any major changes, except that the percentage of energy captured by each mode was reduced. For all three cross-stream planes, the total energy captured by the same numbers of modes was higher in the scalar approach than in the vector approach. Similar changes were also observed for the other two velocity components. The results are consistent with the findings of Freund and Colonius[16] of a smaller energy fraction capture by leading-order modes for vector approach relative to that from scalar approach

Reconstruction of the Flow Dynamics

Time coefficients for each POD spatial eigenfunction computed were obtained by projecting the instantaneous velocity field onto the basis functions using Eq. (5). For quantitative comparisons, Figures 7–9 show the time traces of the longitudinal component of velocity at the lip line of the jet ($r/D = 0.5$) at $x/D = 3$, 6, and 9, for 4 and 12 POD modes, and they are compared with the original velocity. Including only four POD modes allows the capture of the general trend of large amplitude velocity fluctuations due to energetic flow structures. However, the magnitude of large excursions from the mean is much lower than that of the original data, as expected due to the neglect of the higher modes. Using the first eight modes (not shown here)[32] improves the comparison. However, one needs to include in excess of 12 modes to closely match the original results. Similar results were observed for the other two velocity components and also for all three velocity components in the streamwise plane.[32] These results suggest that, with 12 POD modes, the velocity field can be reasonably well reconstructed, and the large-scale structures in the flow can be identified.

Next, a three-dimensional reconstruction of the velocity field, using the first 12 POD modes was performed. A total of 425 snapshots of the 850 available were used, taking every other snapshot, with a time step of 8 μs between consecutive snapshots. The time coefficients, as mentioned before, were calculated by projecting the instantaneous velocity field, the 425 snapshots, onto the POD basis using Eq. (5). Figure 10 compares the original and reconstructed instantaneous streamwise velocity fluctuations at a given time step ($T_s = 116, t = 0.93$ ms) for the cross-stream plane located at $x/D = 3$. The overall comparison is good, but finer details of the original results are smeared out in the reconstruction. Similar

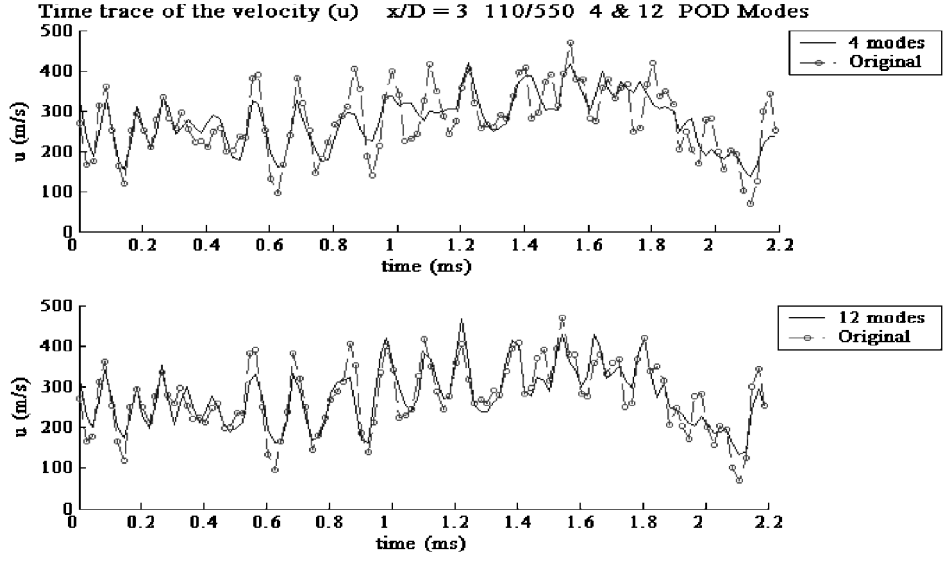

Fig. 7 Time trace of the streamwise velocity component with 4 and 12 POD modes at the nozzle lip line and *x/D* = 3.

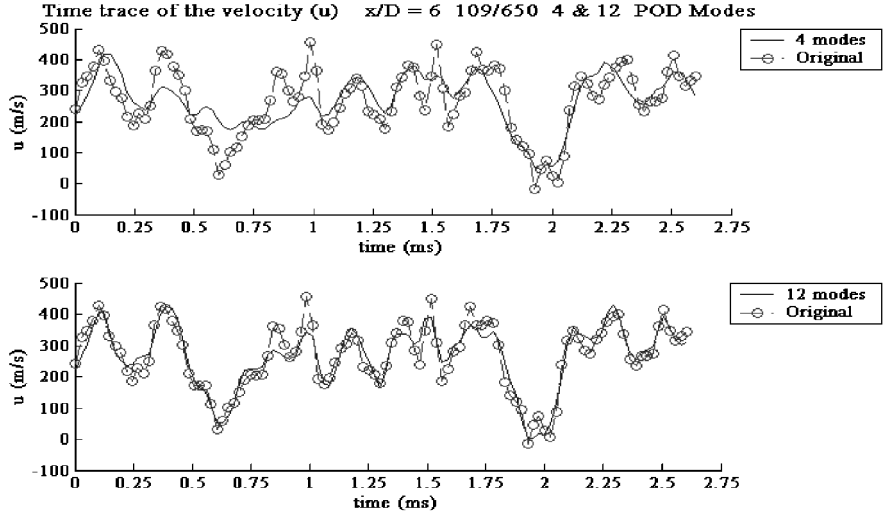

Fig. 8 Time trace of the streamwise velocity component with 4 and 12 POD modes at the nozzle lip line and *x/D* = 6.

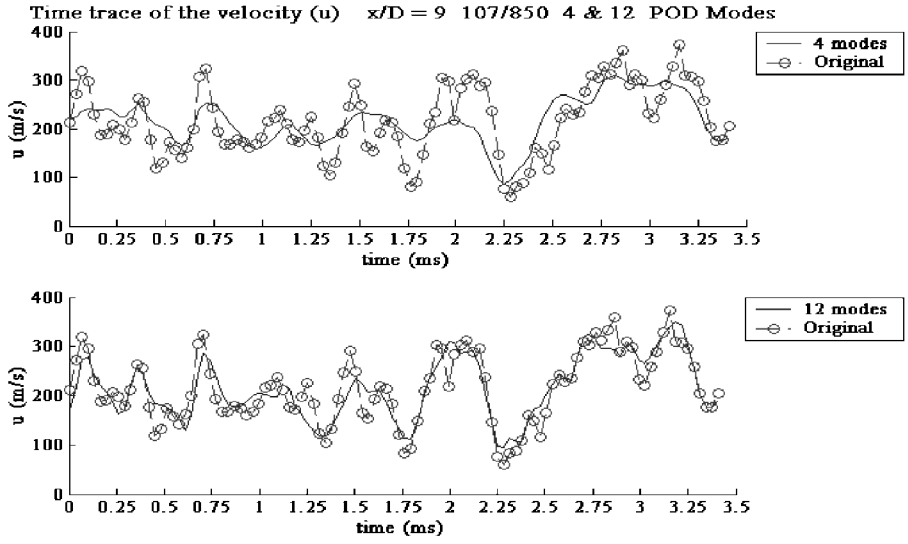

Fig. 9 Time trace of the streamwise velocity component with 4 and 12 POD modes at the nozzle lip line and *x/D* = 9.

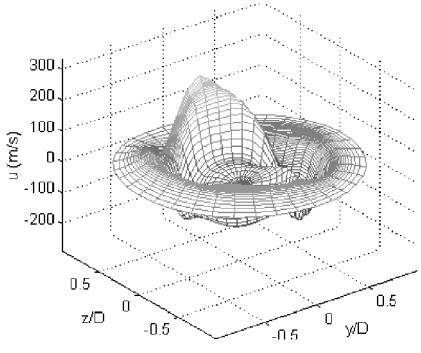

a) Original data

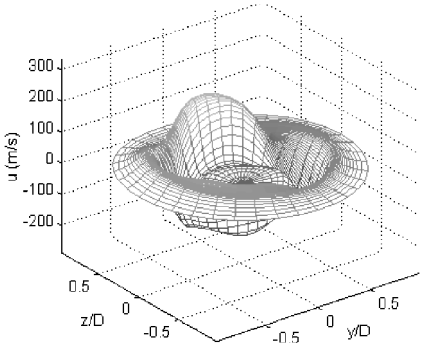

b) 12 POD modes

Fig. 10 Instantaneous streamwise velocity fluctuations at *x/D* = 3: a) original field and b) reconstructed field using 12 POD modes.

agreements are observed at other times as well as in other cross-stream locations.

Animation of the streamwise velocity fluctuations were observed for repeated patterns, similar to the method used by Citriniti and George.[7] To help extract the flow dynamics, the cross-stream velocity vectors (the combined radial and azimuthal velocity components) and the gray scale streamwise vorticity contours along with the streamwise velocity animation were used in each cross-stream plane. Although particular sequences, or a "life cycle" as presented by Citriniti and George[7] in a low-Reynolds-number and low-Mach-number jet were not observed, there was recurrence of certain structures or events that will be shown and discussed hereafter.

Axisymmetric Vortex Ring

The first type of structure observed at the cross-stream plane at $x/D = 3$ is an axisymmetric ring that appears repeatedly, dominating the flowfield. Figure 11 presents a sequence of six frames showing the reconstructed streamwise velocity fluctuations along with the cross-stream velocity vectors and streamwise vorticity contours at $x/D = 3$. The frames are presented in time steps with consecutive time steps having a real time difference of 8 μs. This sequence of streamwise velocity fluctuation images clearly captures the passage of an axisymmetric structure through the plane. The streamwise vorticity contours show negligible vorticity level and the vector plots show primarily radial velocities pointing either inward or outward. Such behavior implies a vortex ring type of structure. The ring starts to affect the flowfield on this plane at $T_s = 20$, and its effect reaches a maximum at around $T_s = 24$. This type of event has been observed before by Citriniti and George,[7] who referred to it as a "volcano-like structure." This type of structure is observed to repeat itself quite often and is clearly related to the first two POD modes ($m = 0$ azimuthal modes) shown in Fig. 3.

Helical Vortex Structure

The second type of structure observed in the reconstructed movies seems to rotate in the azimuthal direction while passing through the $x/D = 3$ plane. Figure 12 shows a set of frames of the reconstructed streamwise velocity fluctuations images, depicting what seems to be a clockwise rotating helical structure. The streamwise vorticity contours, along with the cross-stream velocity vectors at the same time steps show two regions of streamwise vorticity: a much higher positive region and a lower negative region. The positive vorticity region rotates along with the cross-plane velocity component, in the same direction as the helical structure. This type of structure is related to the third POD mode ($m = \pm 1$ azimuthal mode) shown in Fig. 3. An interesting observation is that helical structures in such flows are known to appear farther downstream. However, these results indicate that they could also be present farther upstream, but with less frequent occurrence. Simple visualizations, perhaps, cannot extract their presence. In fact, there were hints of the presence of such structures in a similar upstream location in recent experiments.[18]

Three-Dimensional Structures

Another type of event observed in the reconstructed movies can be associated with three-dimensional structures. A sequence of images showing the presence of large peaks and valleys associated with large-scale structures in the flow are shown in Fig. 13. Streamwise vorticity contours along with cross-stream velocity vector fields show pairs of counter-rotating vortices entraining fluid into the

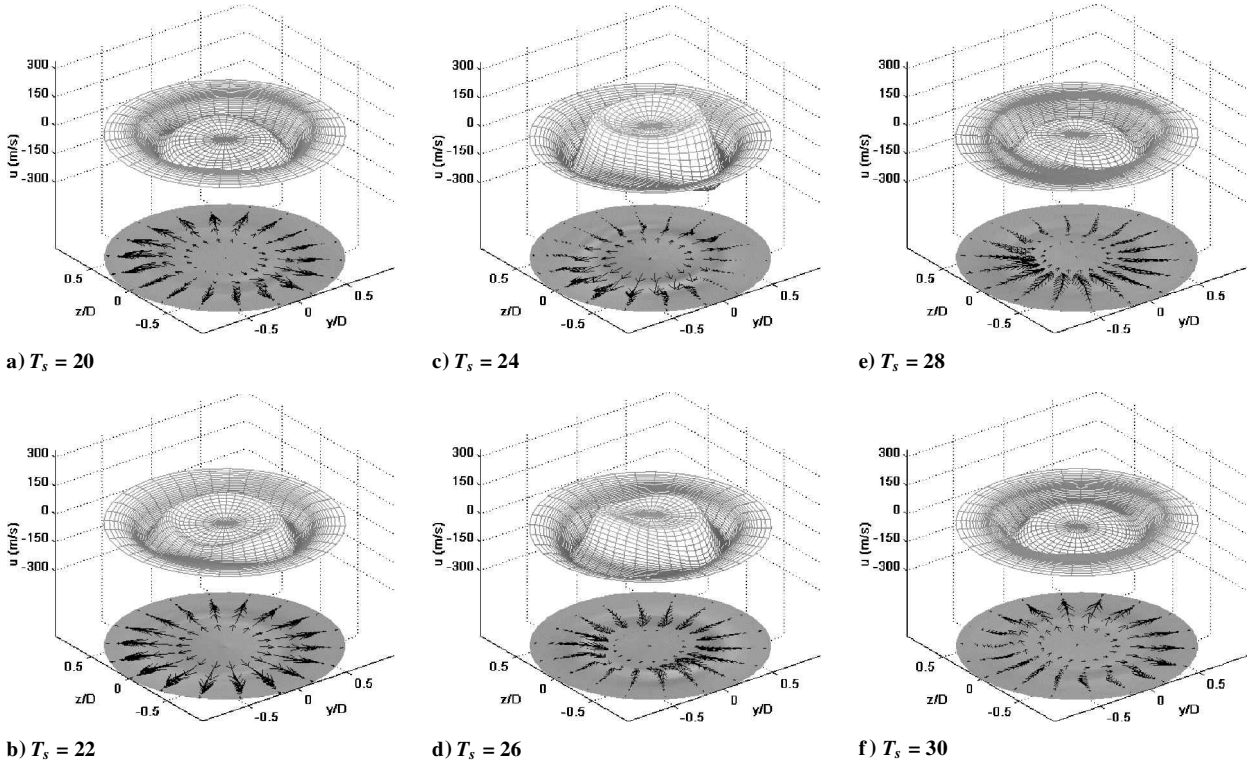

a) T_s = 20 c) T_s = 24 e) T_s = 28

b) T_s = 22 d) T_s = 26 f) T_s = 30

Fig. 11 Three-dimensional reconstructions of the flow at different time steps using 12 POD modes showing the passage of an axisymmetric vortex ring: a)–c) streamwise velocity fluctuations and d)–f) combined cross-stream velocity vectors and streamwise vorticity contours.

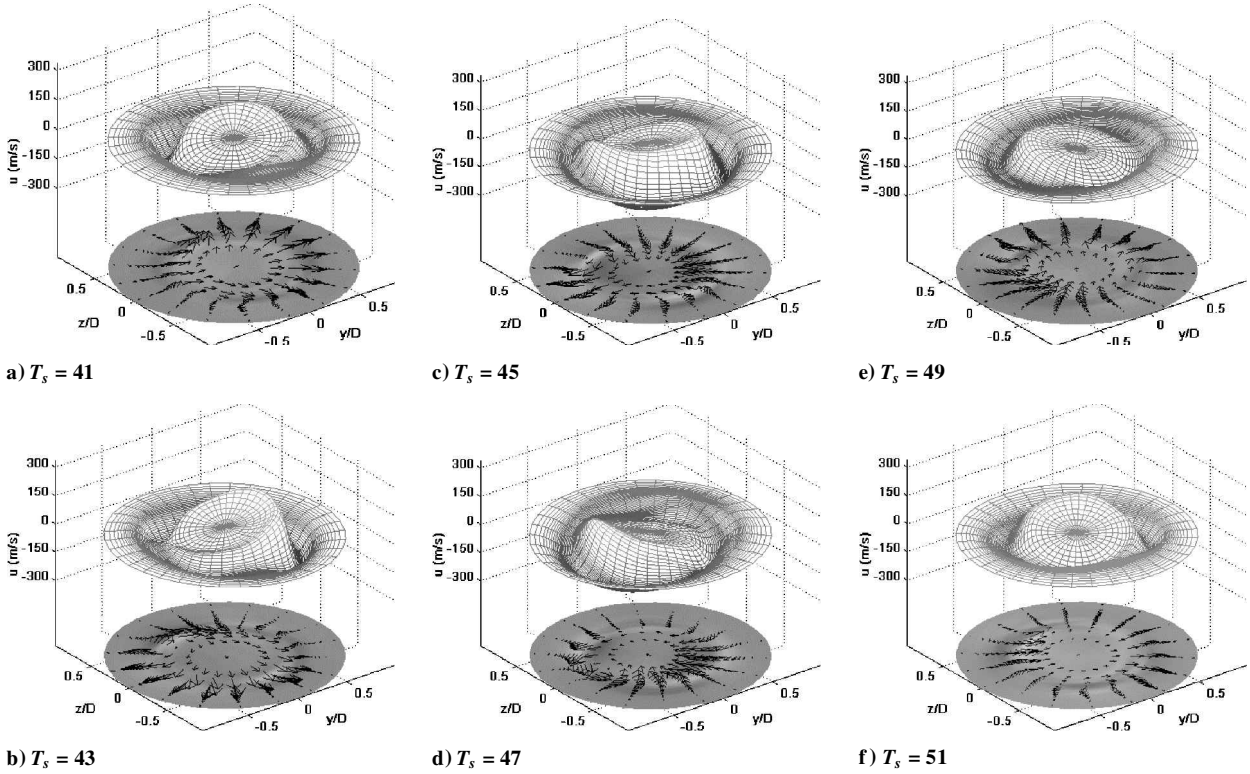

a) T_s = 41 c) T_s = 45 e) T_s = 49

b) T_s = 43 d) T_s = 47 f) T_s = 51

Fig. 12 Three-dimensional reconstructions of the flow at different time steps using 12 POD modes showing the passage of an asymmetric structure (perhaps a helical structure): a)–c) streamwise velocity fluctuations and d)–f) combined cross-stream velocity vectors and streamwise vorticity contours.

regions of high streamwise velocity fluctuations. Such structures are prevalent in flow visualization results of a Mach 1.3 ideally expanded axisymmetric jet.[17] Note that the streamwise vorticity associated with these counter-rotating vortices are much stronger than those associated with the flowfield of Fig. 12. In addition to these three types of events at the cross-stream plane located at $x/D = 3$, there are periods in which there is no clear dominance of any one particular type of structure.

Identification of specific structures using similar three-dimensional constructions at the other two cross-stream planes, $x/D = 6$ and 9, is much more difficult because the structures are more complex. At the $x/D = 6$ plane, more random and three-dimensional behavior of the structures was observed. There was no clear presence of axisymmetric vortex rings; however, vortices of perhaps higher modes ($m = \pm 2, 3$) appear at times. At the $x/D = 9$ plane, the structures are three-dimensional and larger, with slower

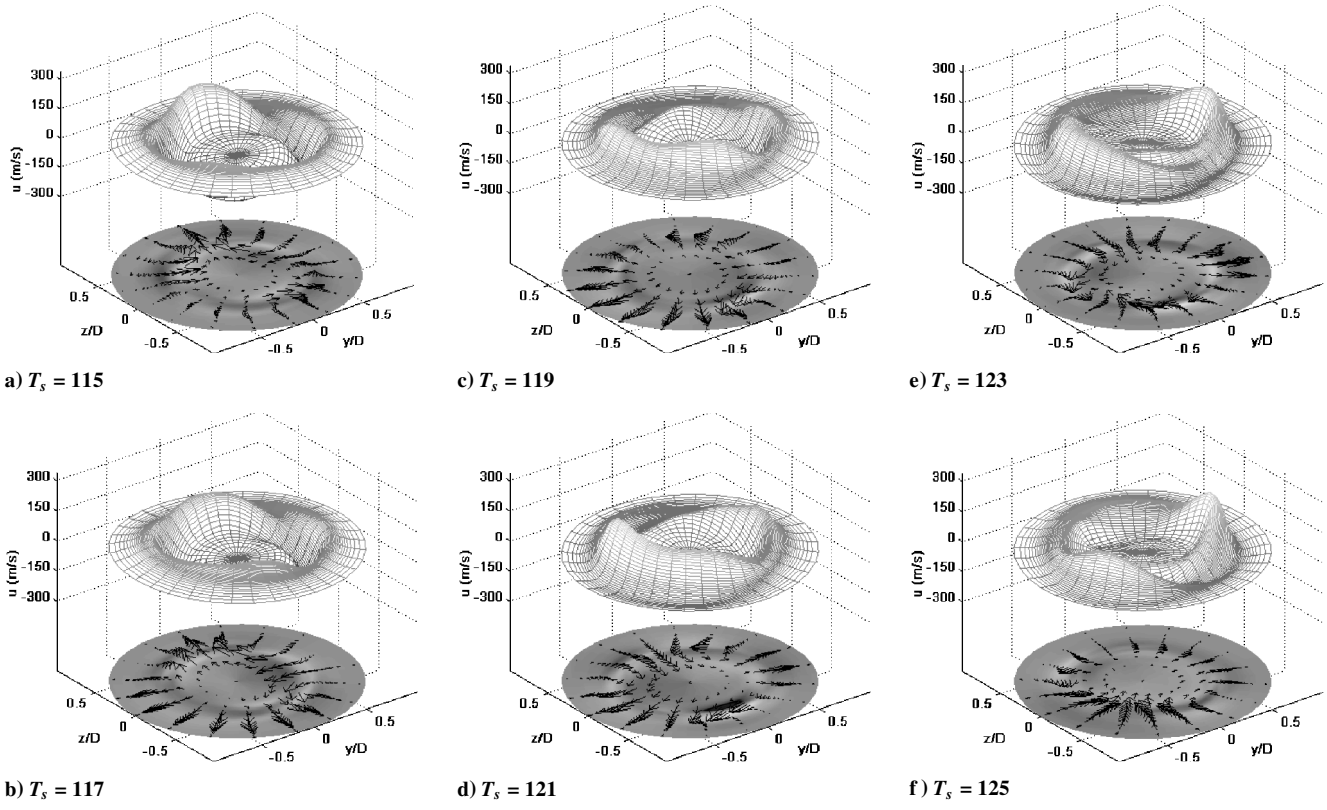

Fig. 13 Three-dimensional reconstructions of the flow at different time steps using 12 POD modes showing the passage of a vortex pair: a)–c) streamwise velocity fluctuations and d)–f) combined cross-stream velocity vectors and streamwise vorticity contours.

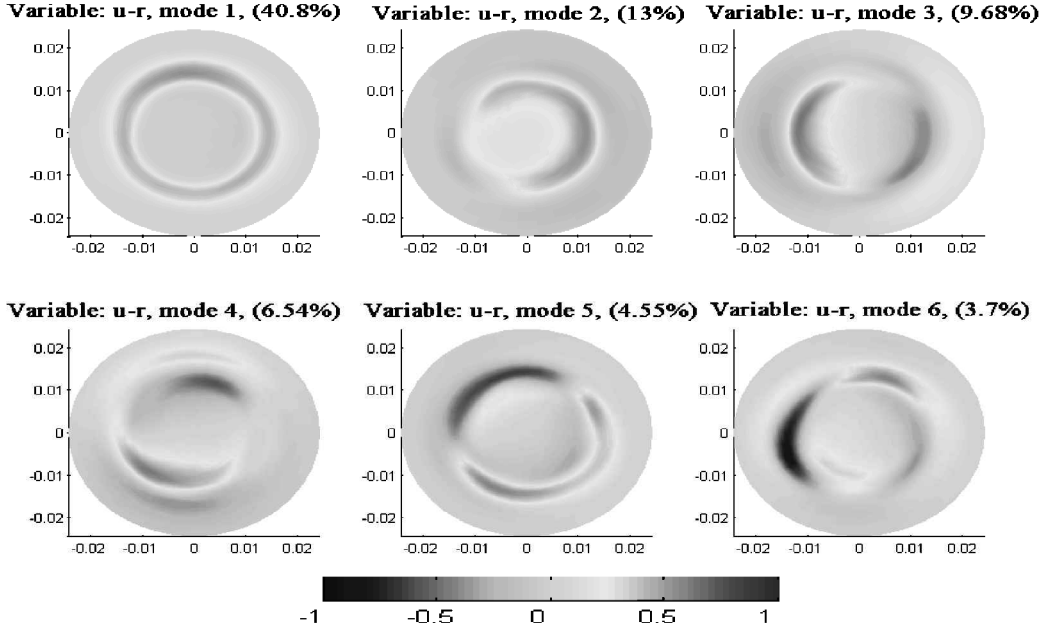

Fig. 14 First six POD modes for the streamwise velocity fluctuations at x/D = 3, using the random data set.

evolution and more spatial homogeneity of properties over the cross plane.

When the flow was reconstructed using the vector POD modes, similar structures were observed. However, there was some loss of the finer details. This was expected because the energy of the modes has changed along with a change in the order of the modes, which would cause some differences in the time coefficient for the vector and the scalar cases. In the context of the jet flow, it appears that the scalar approach might be sufficient in capturing the main characteristics of the flow structures.

Random Temporal Sampling Results: POD Basis and Flow Dynamics

As was mentioned before, two consecutive snapshots in the ordered data sets used to calculate the POD basis are weakly time correlated. However, the data used for POD cover from 40 to 100 convective timescales and, thus, the use of snapshot method should

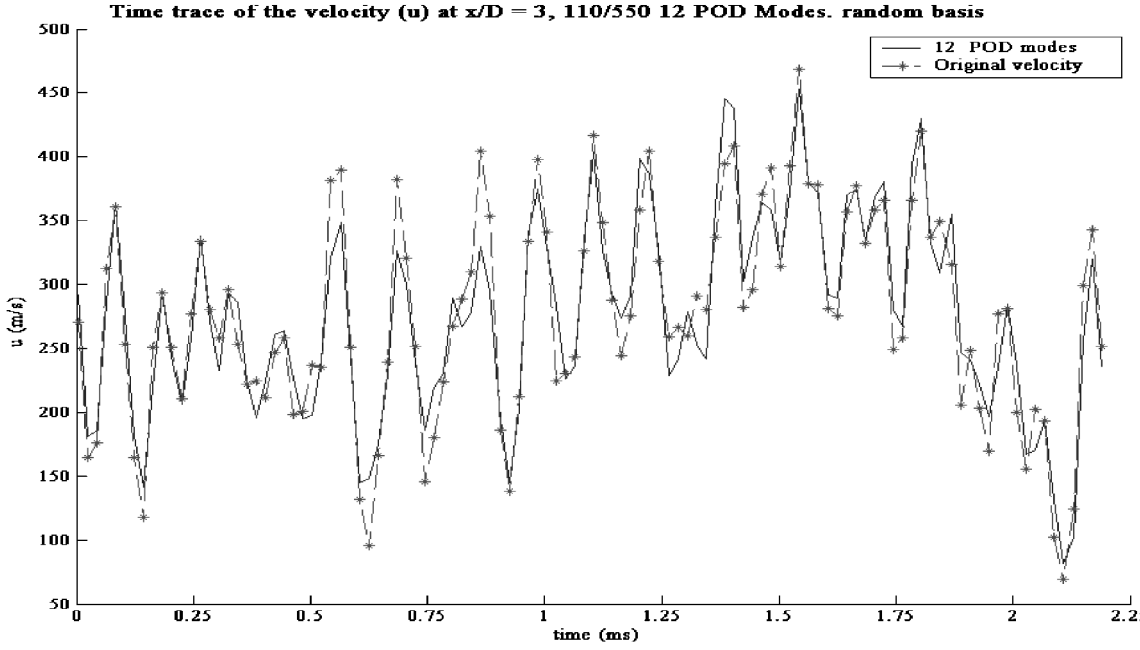

Fig. 15 Time trace of the streamwise velocity component with 12 POD modes at $x/D = 3$, using the random data set.

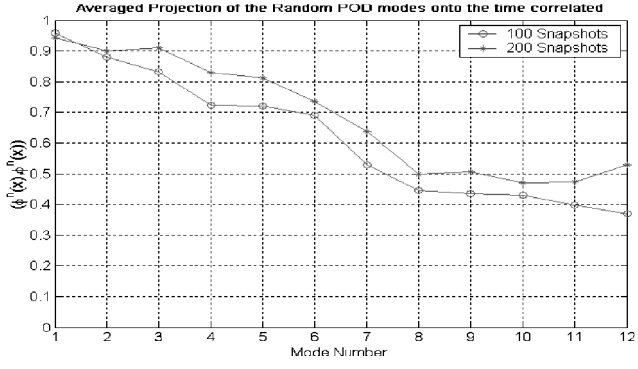

Fig. 16 Averaged projection of the POD modes form random data set onto the POD modes from the ordered data set.

be justified. This should be clear from the good comparison of the reconstructed and original results in Figures 7–10. To further verify this, a set of 100 time steps out of the 850 LES data files available was randomly sampled. The POD modes of this set, from now on called "random data set," were calculated using the snapshot method and are shown in Fig. 14, for the cross-stream plane at $x/D = 3$. Comparing these modes with those obtained using the ordered data set (Fig. 3) reveals that there is little change in the shape of the first four modes or spatial basis, with small variations in the amount of energy captured by each mode. Similarly good comparisons were also observed for the $x/D = 6$ and 9 planes.

Additionally, because the LES data are time resolved, the time coefficients for a given time record length, were obtained by projecting the instantaneous velocity field $u(\boldsymbol{x}, t)$ onto the spatial basis $\varphi^n(\boldsymbol{x})$ calculated from the random data set, using Eq. (5). This time coefficient was used together with the POD basis calculated for the random data set to reconstruct the flowfield, using Eq. (4). The reconstructed longitudinal velocity component using 12 modes at the jet lip line at $x/D = 3$ is compared with the original data in Fig. 15. The comparison is quite good. Similar favorable comparisons were also observed in the $x/D = 6$ and 9 planes.

A more quantitative comparison between the POD modes calculated from the random data set and the ordered data set was obtained by projecting each POD mode of the random data set onto its correspondent mode in the ordered data set, $[\phi_r^n(\boldsymbol{x}), \phi_o^n(\boldsymbol{x})]$. When the value of this projection is closer to one, the two modes are considered very similar and, therefore, the two bases can be ensured to span similar subspaces. This is a more stringent check of the "similarity" of the subspaces spanned by the POD modes, compared to verification of a near-zero angle between the two subspaces (using a set of the respective leading-order POD modes). Figure 16 shows the result of projecting the first 12 POD modes for sets of 100 and 200 snapshots. Note that the results are spatially averaged over 30 sets for each case. Two observations can be made. First, when the number of snapshots is increased (increasing the sample size), there is an improvement in the averaged projection of the modes. Second, from the set of 200 snapshots, the projection of the first three modes is over 0.9, and the first five modes over about 0.8, implying similar modes and a consequently similar subspace (spanned by the leading modes) as the ordered data set. These results suggest that although the higher modes are different between the two cases, the most dominant modes are essentially spanning a similar subspace and should capture the dynamics of the flow.

The real-time measurements to calculate POD time coefficients (combined with the POD basis functions) will be obtained in the future using a real-time PDV technique, which is currently under development.[18] Because of limitations with the laser and camera for such a system, the real-time measurements will be limited to a time period on the order of a convective timescale. The issue of whether this is sufficient for computing time coefficients is explored here. Figure 17 shows the reconstruction of time trace of the velocity at the lip line using the time coefficient calculated with the entire set (850 time steps) and the time coefficient calculated with the 17 time steps (with $\Delta t = 8$ μs) over two portions of the entire time domain (around $t = 0.8$ and 1.8 ms). In both cases, the time coefficient was calculated by projecting the instantaneous snapshots onto the POD basis obtained from the ordered data set using Eq. (5). It can be seen that the results obtained in both cases compare well with the case using the entire data set. This again is encouraging and suggests that one could perhaps use several such time segments to extract a low-dimensional model. However, this process requires further exploration. This route is preferred over the use of projection of Navier–Stokes equations onto the eigenvalues obtained via a standard PDV technique because this will require simultaneous velocity with pressure and density data. Currently, such multiple variable data can be obtained at a point but not on a plane.[36]

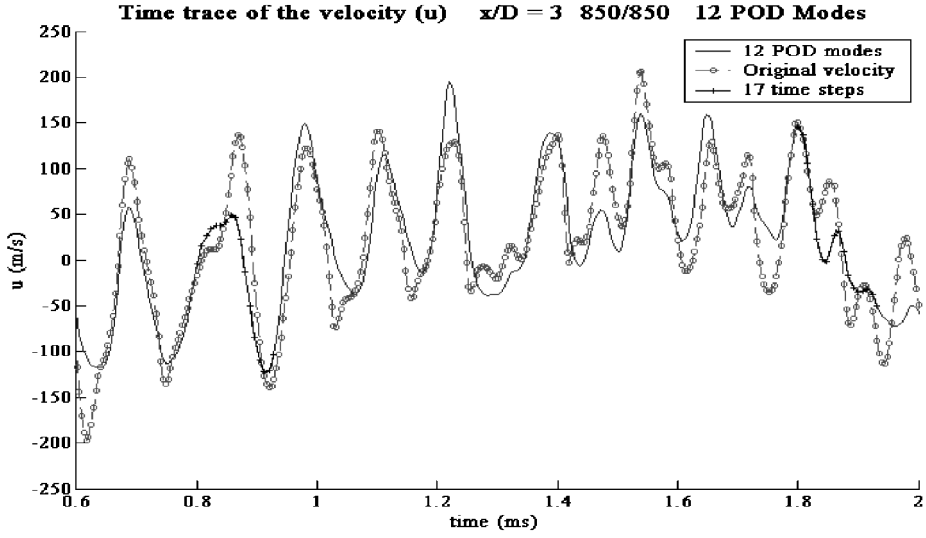

Fig. 17 Comparison of the time trace of the streamwise velocity component at $x/D = 3$ in original data set with 12 POD modes using all of the data set (850 files) and only two small segments of data set.

Conclusions

The snapshot POD technique was used with LES data obtained for an ideally expanded $M = 1.4$ axisymmetric jet. The snapshots used span 40–100 convective time segments. Whereas consecutive snapshots are weakly time correlated, the correlation level drops over a few snapshots, and there is a sufficient number of structures over which the POD modes and time coefficients are calculated. The POD basis calculated at each cross-stream plane using a randomly selected (time uncorrelated) data set showed that the amount of energy captured by different modes, as well as the shape of the modes obtained, did not change measurably in comparison with those obtained using the ordered data set. Although this has not been explicitly addressed in the open literature, this is to be expected from the use of the snapshot method (traditionally used with time uncorrelated data).

The reconstruction of the time traces of the velocity inside the jet shear layer showed that 12 POD modes are sufficient to represent the dynamic flowfield at several locations, with eight modes being sufficient farther upstream. The use of vector POD (velocity fluctuation vector) instead of scalar POD (just streamwise velocity fluctuations) did reduce the energy captured in the first few modes and also changed their rank order, but it did not substantially alter the reconstructed flow. It was found that, in the early jet development region, the first and dominant mode was found to be axisymmetric, followed by either another axisymmetric or asymmetric (probably helical) mode, whereas higher modes in this region and all of the modes farther downstream were more complex and three dimensional. The amount of energy captured by the first POD mode in the cross-stream planes reduces as we approach the end of the potential core, but increases farther downstream, suggesting a process of disorganization/breakdown of initially axisymmetric coherent structures in the interaction region (around the end of the jet potential core) and their reorganization into three-dimensional coherent structures farther downstream. Reconstruction of time evolution of modes confirmed the presence of three different types of structures at the cross-stream plane located at $x/D = 3$; an azimuthal vortex, an apparent helical structure, and a three-dimensional structure associated with vortex pairs. However, the structures farther downstream were observed to be more three dimensional and not amenable to a simple description.

The results are quite encouraging for the use of combined PDV and POD to further explore the physics of high-speed flow and to make an attempt to construct low-dimensional models of the flow. It looks as through one could use standard PDV to determine eigenmodes and real-time short duration PDV to obtain time coefficients.

Acknowledgments

The support of the U.S. Air Force Office of Scientific Research with John Schmisseur and Steven Walker as the Technical Monitors for the work at Gas Dynamics and Turbulence Laboratory at The Ohio State University and also at United Technologies Research Center is greatly appreciated. Fruitful discussions with Lawrence Ukeiley and Thomas Barber are very much appreciated.

References

[1]Lumley, J., "The Structure of Inhomogeneous Turbulent Flows," *Atmospheric Turbulence and Wave Propagation,* Nauka, Moscow, 1967, pp. 166–176.

[2]Sirovich, L., "Turbulence and the Dynamics of Coherent Structures, Part I,II,III: Coherent Structures," *Quarterly of Applied Mathematics*, Vol. 45, No. 3, 1987, pp. 561–590.

[3]Seiner, J., "A New Rational Approach to Jet Noise Reduction," *Theoretical and Computational Fluid Dynamics*, Vol. 10, 1998, pp. 373–383.

[4]Aubry, N., Holmes, P., Lumley, J. L., and Stone, E., "The Dynamics of Coherent Structures in the Wall Region of a Turbulent Boundary Layer," *Journal of Fluid Mechanics*, Vol. 192, 1988, pp. 115–173.

[5]Glauser, M., and George, W., "An Orthogonal Decomposition of the Axisymmetric Jet Mixing Layer Utilizing Cross-Wire Velocity Measurements," *Proceedings of the Sixth Symposium on Turbulent Shear Flow*, Toulouse, France, 1987, pp. 10.1.1–10.1.6.

[6]Glauser, M., Zheng, X., and George, W., "The Streamwise Evolution of Coherent Structures in the Axisymmetric Jet Mixing Layer," *Symposium on Recent Developments in Turbulence*, Springer-Verlag, New York, 1990, pp. 207–222.

[7]Citriniti, J., and George, W., "Reconstruction of the Global Velocity Field in the Axisymmetric Mixing Layer Utilizing the Proper Orthogonal Decomposition," *Journal of Fluid Mechanics*, Vol. 418, 2000, pp. 137–166.

[8]Ukeiley, L., and Seiner, J., "Examination of Large Scale Structures in a Transonic Jet Mixing Layer," *Proceedings of FEDSM'98*, Washington, DC, 1998.

[9]Delville, J., Ukeiley, L., Cordier, L., Bonnet, J. P., and Glauser, M. "Examination of Large-Scale in a Turbulent Plane Mixing Layer. Part 1. Proper Orthogonal Decomposition" *Journal of Fluid Mechanics*, Vol. 391, 1999, pp. 91–122.

[10]Gordeyev, S., and Thomas, F., "Coherent Structure in the Turbulent Planar Jet. Part 1. Extraction of the Proper Orthogonal Decomposition Eigenmodes and Self-Similarity," *Journal of Fluid Mechanics*, Vol. 414, 2000, pp. 145–194.

[11]Khibnik, A. I., Narayanan, S., Jacobson, C. A., and Lust, K., "Analysis of Low Dimensional Dynamics of Flow Separation," *Notes on Numerical Fluid Mechanics*, edited by D. Henry and A. Bergeon, Vol. 74, Vieweg Verlag, Brunswick, Germany, 2000, pp. 167–178.

[12]Rowley, C. W., Colonius, T., and Murray, R., "POD Based Models of Self-Sustained Oscillations in the Flow past an Open Cavity," AIAA Paper 2000-1969, June 2000.

[13]Rowley, C. W., Colonius, T., and Murray, R., "Dynamical Models for Control of Cavity Oscillations," AIAA Paper 2001-2126, May 2001.

[14]Ukeiley, L., Seiner, J., Srinivasan, A., Sinha, N., and Dash, S., "Low-Dimensional Description of Resonating Cavity Flow," AIAA Paper 2000-2459, June 2000.

[15]Ukeiley, L., Whitten, J., Kannepalli, C., Srinivasan, A., and Sinha, N., "Low-Dimensional Description of Variable Density Flows," AIAA Paper 2001-0515, Jan. 2001.

[16]Freund, J. B., and Colonius, T., "POD Analysis of Sound Generation by a Turbulent Jet," AIAA Paper 2002-0072, Jan. 2002

[17]Samimy, M., and Wernet, M. P., "Review of Planar Multiple-Component Velocimetry in High-Speed Flows," *AIAA Journal*, Vol. 38, No. 2, 2000, pp. 553–574.

[18]Thurow, B., Hileman, J., Samimy, M., and Lempert, W., "Compressibility Effects on the Growth and Development of Large-Scale Structures in an Axisymmetric Jet," AIAA Paper 2002-1062, Jan. 2002.

[19]Thurow, B., Hileman, J., Samimy, M., and Lempert, W., "Progress Towards a Real-Time Quantitative Measurement Technique for High-Speed Flows," AIAA Paper 2001-2985, June 2001.

[20]Lumley, J., "Coherent Structure in Turbulence," *Transition and Turbulence*, edited by R. E. Meyer, Mathematics Research Center Symposia and Advanced Seminar, Academic Press, New York, 1981, pp. 215–242.

[21]Berkooz, G., Holmes, P., and Lumley, J. L., "The Proper Orthogonal Decomposition in the Analysis of Turbulent Flows," *Annual Review of Fluid Mechanics*, Vol. 25, 1993, pp. 539–575.

[22]Delville, J., Cordier, L., and Bonnet, J. P., "Large-Scale-Structure Identification and Control in Turbulent Shear Flows," *Flow Control: Fundamentals and Practice*, edited by M. Gad-el-Hak, A. Pollard, and J. Bonnet, Springer-Verlag, New York, 1998, pp. 199–273.

[23]DeBonis, J. R., and Scott, J. N., "Large-Eddy Simulation of a Turbulent Compressible Round Jet," *AIAA Journal*, Vol. 40, No. 7, 2002, pp. 1346–1354.

[24]DeBonis, J. R., and Scott, J. N., "Study of the Error and Efficiency of Numerical Schemes for Computational Aeroacoustics," *AIAA Journal*, Vol. 40, No. 2, 2002, pp. 227–234.

[25]Carpenter, M. H., and Kennedy, C. A., "Fourth-Order 2N-Storage Runge–Kutta Schemes," NASA TM 109112, 1994.

[26]Kennedy, C. A., and Carpenter, M. H., "Comparison of Several Numerical Methods for Simulation of Compressible Shear Layers," NASA TP 3484, 1997.

[27]Moin, P., Squires, K., Cabot, W., and Lee, S., "A Dynamic Subgrid-Scale Model for Compressible Turbulence and Scalar Transport," *Physics of Fluids A*, Vol. 3, No. 11, 1991, pp. 2746–2757.

[28]DeBonis, J. R., "The Numerical Analysis of a Turbulent Compressible Jet," Ph.D. Dissertation, Dept. of Aerospace Engineering and Aviation, Ohio State Univ., Columbus, OH, Dec. 2000.

[29]Panda, J., and Seasholtz, R. G., "Velocity and Temperature Measurement in Supersonic Free Jets Using Spectrally Resolved Rayleigh Scattering," AIAA Paper 99-0296, Jan. 1999.

[30]Caraballo, E., Samimy, M., Narayanan, S., DeBonis, J., and Scott, J., "Application of Proper Orthogonal Decomposition to a High-Speed Axisymmetric Jet," AIAA Paper 2001-2783, June 2001.

[31]Hayakawa, M., and Hussain, F., "Three Dimensionality of Organized Structures in a Plane Turbulent Wake," *Journal of Fluid Mechanics*, Vol. 206, 1989, pp. 375–404.

[32]Caraballo, E., "An Application of the Proper Orthogonal Decomposition to an Axisymmetric Supersonic Jet," M.S. Thesis, Dept. of Mechanical Engineering, Ohio State Univ., Columbus, OH, April 2001.

[33]Hileman, J., and Samimy, M., "Turbulence Structures and the Acoustic Far-Field of a Mach 1.3 Jet," *AIAA Journal*, Vol. 39, No. 9, 2001, pp. 1716–1727.

[34]Hileman, J., Thurow, B., and Samimy, M., "Exploring Noise Sources in a Mach 1.3 Jet via Simultaneous Acoustic Measurements and Temporally Resolved Flow Visualizations," *AIAA Journal*, Vol. 40, No. 12, 2002, pp. 2382–2392.

[35]Corke, T. C., Shakib, F., and Nagib, H. M., "Mode Selection and Resonant Phase Locking in Unstable Axisymmetric Jets," *Journal of Fluid Mechanics*, Vol. 223, 1991, pp. 253–311.

[36]Elliott, G. S., and Samimy, M., "Rayleigh Scattering Technique for Simultaneous Measurements of Velocity and Thermodynamics Properties," *AIAA Journal*, Vol. 34, No. 11, 1996, pp. 2346–2352.

R. P. Lucht
Associate Editor